Electronic Supplementary Material (ESI) for Physical Chemistry Chemical Physics.
This journal is © the Owner Societies 2021

Supplementary Information for

An Atomistic View of Solvent-Free Protein Liquids: The Case of Lipase A

Sudarshan Behera,[a] Sudip Das [a] and Sundaram Balasubramanian [*a]

[a]*Chemistry and Physics of Materials Unit*

Jawaharlal Nehru Centre for Advanced Scientific Research, Bangalore 560 064, India

E-mail: bala@jncasr.ac.in

Table of Contents

1. Definitions and Explanations

1.1 Why were 27 surfactants considered per enzyme? 4

1.2 Lifetime correlation function for the N-C pair 4

1.3 Time autocorrelation function for bond vector 4

1.4 β(t) exponent 4

1.5 Initial structure of the surfactant 5

1.6 Comparison of average RDFs 5

1.7 Aligning Enzymes 5

1.8 Protocol for pair energy calculation 5

2. Additional Computational Details 5

3. Supplementary Results

3.1 Results from the simulation of [cLipA:nS] 6

3.2 Pair energy distribution 6

3.3 Comparison of Number of H-bonds between WT LipA and SFPL-64 7

4. Supplementary Movies

4.1 Comparing structural dynamics of LipA (SM1.mp4) 7

4.2 Transition of a water between two enzymes (SM2.mp4) 7

5. Supplementary Figures

5.1 S1 8

(A) Cationized Aspartate and Glutamate

(B) Initial Structure of [cLipA:27S]

(C) Final Structure of [cLipA:27S]

(D) Electrostatic potential surface the cationized enzyme (cLipA)

(E) All atom RMSD value of enzyme against simulation time

(F) Radius of Gyration as a function of simulation time

5.2 S2. Amber atom types of cationized aspartate and glutamate 9

5.3 S3. 10

(A) Pair energy distributions of various pairs in SFPL-64

(B) vdW and electrostatic contributions to surfactant-surfactant interactions

(C) vdW and electrostatic contributions to enzyme-surfactant interactions

(D) Pair energy distribution of water

(E) Pair energy distribution of argon

5.4 S4. Comparison of average RDFs 11

5.5 S5. Snapshots of pairs of enzyme-surfactant complexes showing interdigitation of surfactants 11

5.6 S6. g(r) and running coordination number of non-hydrogen atoms of inter-complex surfactants 12

5.7 S7. Comparison of End-to-End Distance of Surfactant 12

5.8 S8 13

(A) RMSF of backbone atoms of LipA in aqueous and SFPL-64 system

(B) RMSF of side chain atoms of LipA in aqueous and SFPL-64 system

5.9 S9. Examples of surfactant alkyl interacting with one enzyme 14

5.10 S10. Examples of surfactant alkyl interacting with two enzymes 15
5.11 S11. Number of surfactants, a protein interacts with 16
5.12 S12. Lifetime Correlation Function of N-C pair 16
5.13 S13 17
(A), (B) Density isosurfaces of surfactant PEG
(C), (D) Density isosurfaces of surfactant alkyl
5.14 S14. Alkyl density present near certain protein residues 18
5.15 S15. Snapshots of two independent SFPL-64 19
5.16 S16 MSD plots of Protein COM and various parts of the surfactant 19
5.17 S17. Comparison of TCFs of bond vectors from SFPL-27 and SFPL-64 20
5.18 S18. TCFs of side chain bond vectors of different segments 20
5.19 S19. TCFs of backbone bond vectors of different segments 21
5.20 S20 22
(A) RDFs of oxygen atom of water with different atoms
(B) Running Coordination number of oxygen atom of water with different atoms
5.21 S21 22
(A) MSDs of different types of water molecules
(B) β(t) exponent of the all and non-buried water molecules
5.22 S22 23
(A1) Trajectory of a water molecule transits from one enzyme to another
(A2) Distance of the same water molecule from COM of left enzyme against time
(B1), (B2) Same as (A1) and (A2), but for another water molecule
5.23 S23. Snapshots of oxygen atom of a transiting water 24
5.24 S24 25
(A) A water molecule changing its protein identity
(B) Zoomed view of Panel (A)
(C) Fraction of atom types around a water molecule as a function of simulation time
5.25 S25 26
(A) Surfactant head groups in SFPL-64
(B) Surfactant alkyl groups in SFPL-64
5.26 S26 26
(A) Mean squared displacement: Comparison between SFPL and SFPL-noW
(B), (C) TCFs of bond vectors: Comparison between SFPL and SFPL-noW

1. Definitions and Explanations

1.1 Why were 27 surfactants per enzyme considered for solvent-free liquid modeling?

Experimentally, the unbound surfactant molecules from the aqueous solution of cLipA were removed by dialysis, and the number of surfactants bound per enzyme was found to be 38±1[1]. Since there are only 27 surfactant binding sites, whether all the 38±1 surfactants are bound to the enzyme surface was a doubt. To investigate this, we calculated the solvent-accessible surface area (SASA) of cationized LipA and showed that there is no significant increase in SASA going from 39 to 31 surfactants (SI Table-S1). Thus, all the 38±1 are not directly bound to the enzyme surface. Some of them may be simply a part of the PEG aggregate structures formed on the enzyme surface and may not have been removed via dialysis. In other protein liquids[2], it has been reported that the number of surfactants bound per enzyme is the same as the number of surfactant binding sites. Thus, 27 surfactants per enzyme were taken in constructing the model of the solvent-free liquid in our simulations.

Table-S1. Protein SASA

S. No.	System	Protein SASA (nm^2)
1	cLipA	97.6 ± 1.6
2	[cLipA:39S]	44.6 ± 1.4
3	[cLipA:33S]	45.2 ± 1.4
4	[cLipA:31S]	45.0 ± 2.3
5	[cLipA:30S]	54.8 ± 1.8
6	[cLipA:27S]	55.5 ± 1.9

1.2 Lifetime Correlation Function of N-C pair

The dynamic behavior of the N-C pair can be analyzed by calculating the time autocorrelation function of the pair which is given by,

$$C_x(t) = \left\langle \frac{\sum h_{ij}(t_0) h_{ij}(t_0 + t)}{\sum h_{ij}(t_0)^2} \right\rangle \tag{1}$$

Where h_{ij} is a binary measure of whether the pair is attached or detached. If the distance between N and C of a pair is less than 5 Å, it is attached, and hence $h_{ij} = 1$ or else it is detached and $h_{ij}=0$. The summation is performed over all the pairs, and the angular brackets represent an average over many different time origins in the trajectory. The subscript x refers to the two different definitions for measuring h_{ij} at future points in time, continuous or intermittent. In the continuous case, once an N-C pair is detached, it is always considered as detached even if the pair gets attached subsequently. In the intermittent case, the N-C pair is allowed to be attached, at a future point in time.

1.3 Time Autocorrelation Function of Bond Vector

Gromacs[3] computes the time correlation function for bond vector using the following relation,

$$C_v(t) = \langle \mathrm{P}_n \cos\angle\big(\mathrm{v}(t_0), \mathrm{v}(t_0 + \mathrm{t})\big)\rangle_{t_0} \tag{2}$$

P_n is the nth order Legendre polynomial. n=1 is used in this work. $v(t_0)$ and $v(t_0+t)$ are the bond vectors at time t_0 and t_0+t, respectively.

1.4 β-exponent

To determine if the components of the SFPL were in the diffusive regime, d[log(msd)]/d[log(t)] (called β) is plotted against time, t. For a diffusive system, it has a converged value of 1. If β is < 1, the system is sub-diffusive.

1.5 Initial Structure of the Surfactant

An arbitrarily folded structure of the surfactant was built using GaussView[4] and followed by geometry optimization with Gaussian 09[5] at HF/6-31G* level. The GAFF[6] parameters and RESP[7] partial atomic charges for the optimized geometry were obtained using Antechamber[8] and Acepype[9]. The surfactant was then solvated in a TIP3P[10] water box and subjected to the same energy minimization and equilibration protocols as WT LipA. The equilibrated configuration was simulated for 50ns in the NPT ensemble. Geometry optimization of the structure of the surfactant at the 50 ns time frame was done using the same protocol, and GAFF parameters and RESP charges were obtained. For any further modeling where surfactant molecules were needed, the quantum optimized structure of the surfactant was considered as the initial structure.

1.6 Average P-P g(r) is independent of the initial distribution of enzymes in the simulation box

The P_{com}-P_{com} g(r) presented in the manuscript (Figure 2-A) is averaged over ten independent MD trajectories of SFPL-64 and hence the dependence of the g(r) on the initial distribution of enzymes in the simulation box is unlikely to contribute. To further strengthen this conclusion, three RDFs are compared in SI Figure S3-A. Each of them were obtained as average over just three (out of the ten) different MD trajectories of the SFPL-64 system. The figure also displays the RDF averaged over all the ten runs. The RDFs nicely match each other (leaving aside the statistical noise). As a further evidence, we have also compared the average RDFs obtained from the SFPL-64 and the SFPL-27 systems (SI Figure S3-B), each of them being a mean of RDFs from ten independent MD runs; their close match further supports our faith in the inter-protein RDF of the SFPL system presented in Figure 2-A.

1.7 Aligning Enzymes to obtain Density Isosurfaces of SFT Groups and of Water

The structure of an arbitrarily chosen enzyme from the first time frame of the production run of an independent configuration of SFPL-64 (out of ten independent configurations) is defined as the reference enzyme structure. In order to align the backbone atoms of a chosen enzyme structure, say target, to the backbone atoms of the reference enzyme, a transformation matrix (*vide infra*) is needed. These transformation matrices were then, applied to their corresponding target enzyme structures as well as to all the surfactant and water molecules, whose at least one non-hydrogen atom falls within 5 Å of any non-hydrogen atoms of the target enzyme. These surfactant and water molecules were used further to calculate density values (for the generation of density isosurfaces).

For the calculation of TCFs of bond vectors as well, such a transformation is needed, as the enzyme can rotate during the MD run. Each enzyme of an independent SFPL-64 simulation run has a reference structure which was chosen as its structure in the first time frame. So, there are 64 reference structures in one SFPL-64 simulation run. The corresponding structures of the reference enzymes at future time frames are their targets. Transformation matrices were constructed to align the backbone atoms of the target structures to their reference structures, and were applied on all the atoms of the target enzyme structures. The same protocol was applied to all the independent simulation runs of SFPL-64, with 64 different reference structures in each run.

The construction of transformation matrices and aligning of target structures to reference structures were done using the *align* module, whereas the density values were calculated using *density* module, both of which are part of the MDAnalysis[11] package.

1.8 Protocol for pair energy calculation

An enzyme-surfactant complex is defined to be constituted by an enzyme and the 27 surfactants which are electrostatically bound to it. Later, the pair interaction energy between every possible pair of enzyme-surfactant complexes in SFPL-64 is calculated using the *energy* module of the GROMACS package[3]. Since only a maximum of 64 energy groups can be defined in GROMACS and the whole system is by default considered as one energy group, 63 out of 64 enzyme-surfactants complexes were considered for the energy calculation. Thus, the pair interaction energy was calculated for ${}^{63}C_2$ (=1953) pairs. The same protocol was followed and pair energies were calculated from all the ten independent runs. Enzyme-enzyme, surfactants-surfactants, and enzyme-surfactants pair energies were also calculated from pairs of enzyme-surfactant complexes following the same protocol. The 27 surfactants from an enzyme-surfactant complex are considered as one group while calculating surfactants-surfactants and enzyme-surfactants pair energies.

2. Additional Computational Details

Cationized aspartate and glutamate residues were constructed using GaussView[4] (SI Fig. S1-A). The C-terminal and N-terminal are capped by N-methine amide (NME) and N-acetyl (ACE) groups, respectively. Geometry optimization of these structures were performed with Gaussian 09[5] at HF/6-31G* level of theory. The AMBER atom types (see SI Figure S2) and RESP[7] partial atomic charges for these residues were generated using acpype and antechamber. These partial atomic charges were used for MD simulations within the AMBER99SB-ILDN force field[12], for all the other bonded and nonbonded parameters involving the generated atom types. AMBER99SB-ILDN force field was used for other amino acid residues. Although the AMBER99SB-ILDN force field is parametrized for proteins in the aqueous medium, it has also shown promising results for gas[13] and

crystalline[14] phase simulations of proteins. Hence, we believe that this force field would model the solvent-free protein liquids reasonably well. The surfactants were added to the enzyme surface manually, whereas the 64 and 27 copies of PWS-complex were built using VMD[15] (Tcl) scripting. All the simulations were performed using GROMACS-2018.3 package[3] employing the conjugate gradient algorithm[16] for energy minimization and Leap-frog integrator[17] with 2 fs time step for molecular dynamics simulation, taking three-dimensional periodic boundary condition into account. Solvation was treated with the TIP3P water model[10]. Both coordinates and velocities were dumped every 10ps. During equilibration, the Bussi-Donadio-Parrinello velocity rescaling thermostat[18] and Berendsen barostat[19] were used for temperature and pressure coupling, respectively. The barostat was switched to Parrinello-Rahman[20] for the NPT production runs. LINCS algorithm[21] was used to constrain all the bonds, and PME[22] was used for electrostatic interaction calculations. Both electrostatic and van der Waals interactions were cut off at 10 Å and shifted, and long-range corrections were added to both energy and pressure.

Root-mean-square-deviation (RMSD), root-mean-square-fluctuation (RMSF), secondary structure content, radius of gyration (R_g), radial distribution function (RDF), time autocorrelation functions (TCFs) for bond vectors were calculated using GROMACS-2018.3 in-built modules. Visualizations were done using VMD. Electrostatic potential was generated using the APBS server[23]. Other codes for analyses were written in python using MDAnalysis package[11] and Tcl in VMD. Results are averaged over all the enzymes in a MD trajectory and also over all the independent runs, wherever necessary and available.

For simulating bulk liquid water, 510 water molecules in a 25 Å cubic box was considered as the initial configuration. The water box was subjected to energy minimization, equilibration at NVT (300K) and then NPT (300K and 1 bar) ensemble, and finally a production run for 30 ns in the NPT ensemble. The trajectory from the production run was considered for the pair energy calculation.

Table-S2. Summary of the simulations

Sr. No	Enzyme Form	No. of water molecules	No. of surfac-tants	No. of Protein (s)	Cubic Box length (Å)	Total No. of atoms	No. of indepe-ndent runs	Trajectory length of each run (ns)
1	WT LipA (300K, 1 bar)	8555	0	1	65.7	28,392	3	100
2	WT LipA (333K, 1 bar)	8555	0	1	66.4	28,392	3	100
3	cLipA (300K, 1 bar)	9802	0	1	68.7	32,375	3	100
4	[cLipA:27S] (300K, 1 bar)	62060	27	1	118.7	1,94,792	2	100
5	SFPL-27 (333K, 1 bar)	27x40 =1080	27x27 =729	27	129.7	2,35,764	10	500(1) 100 (9)
6	SFPL-64 (333K, 1 bar)	64x40 =2560	64x27 =1728	64	172.9	5,58,848	10	100
7	SFPL-noW (333K, 1 bar)	0	64x27 =1728	64	172.3	5,51,168	3	100

3. Supplementary Results

3.1 Results from the Simulation of [cLipA:nS]

MD simulations of aqueous [cLipA:27S] show the formation of anionic surfactant aggregates on the enzyme surface (SI Figure S1-C). The surfactants organize themselves on the enzyme surface in such a way that the hydrophilic part interacts either with the positively charged enzyme surface or with water, whereas the hydrophobic alkyl components interact among themselves and form clusters, which are hidden away from water. A large area of the enzyme surface (SASA-57%, SI Table-S1) in [cLipA:27S] is left exposed to water, suggesting that 27 surfactants are not enough in a high dielectric medium such as water to cover the entire enzyme surface with their hydrophilic head part as well as to hide their hydrophobic alkyl tail from the water.

3.2 Pair energy distribution

The distribution of energies of pairs of various kinds (SI Figure S2-A) all show a large peak at zero energy, corresponding to the large number of pairs at large distances. The pairs of enzymes alone in the SFPL displays a short foray into the negative energy values as well. However, the surfactant-surfactant pair energy distribution shows a substantial and broad shoulder centered at -200 kcal/mol, arising from short contacts

between surfactants 'belonging' to different enzymes, via their interdigitated character (SI Figure S3). This interaction energy is likely to be largely van der Waals in character. Although the strength of each contribution to it will be less than 1 kcal/mol, the number of such interactions is rather large (see SI Figure S4 which provides an estimate of this number via a pair correlation function analysis). The combination of the surfactant-surfactant as well as the protein-surfactant interactions contributes to the emergence of a distinct, broad feature spread between -200 and -300 kcal/mol in the complex-complex pair energy distribution, along with a distinct long tail. The protein-surfactant and surfactant-surfactant interaction energies were further broken down into van der Waals and electrostatic contributions (SI Figure S2-B, C). In both cases, the van der Waals contribution to the interaction energy is more stabilizing than the electrostatic interactions. In Figure S2-B and Figure S2-C, we provide pair energy distributions for pairs of water molecules in neat, liquid water (modelled with the TIP3P potential) at ambient conditions, as well as for pairs of argon atoms in liquid argon at 130K and 40 atm pressure. Note the presence of distinct feature at -5 kcal/mol in the case of water, corresponding to hydrogen bonded pairs[24] and -0.24 kcal/mol in the case of argon, corresponding to the interaction strength of an argon atom with each of its 12 near neighbours.

3.3 Comparison of Number of H-bonds between WT LipA and SFPL-64

Table-S3. Number of H-bonds

Enzyme Form	Oxygen of Water/Surfactant as	Whole Protein	Backbone	Side chain
WT LipA	Donor	162±8	87±6	75±5
	Acceptor	84±6	27±3	57±5
SFPL-64	Donor	66±5	9±3	57±5

4. Supplementary Movies

4.1 Comparing structural dynamics of LipA (SM1.mp4)

The full trajectories (100ns) of LipA in aqueous solution and a LipA from SFPL-64 are shown (both the systems are at 333 K). Side chains of two residues (Ile135 and Val154) are shown in orange color for better comparison of side chain dynamics. The movie demostrates the similarity of backbone dynamics in the SFPL and in the aqueous solution.

4.2 Transition of a water between two enzymes (SM2.mp4)

In the movie, enzymes are shown in blue with new cartoon represenations. The transparent red and green color quicksurf representations are for surfactant head and alkyl groups respectively. The Oxygen atom of the water molecule is shown as a magenta ball. The distance between the center of mass of the enzyme on the left hand side and that of water is plotted as function of simulation time in the inset (left corner). This movie shows the transition of a water from one enzyme (present on the left in the movie) to another (right) during the course of simulation. The “superfast” motion of water is observed at around 69 ns. This movie also depicts that the water molecule travels via the PEG-rich hydrophilic regions and, hence avoids the alkyl regions of the surfactant medium during the transit.

5. Supplementary Figures

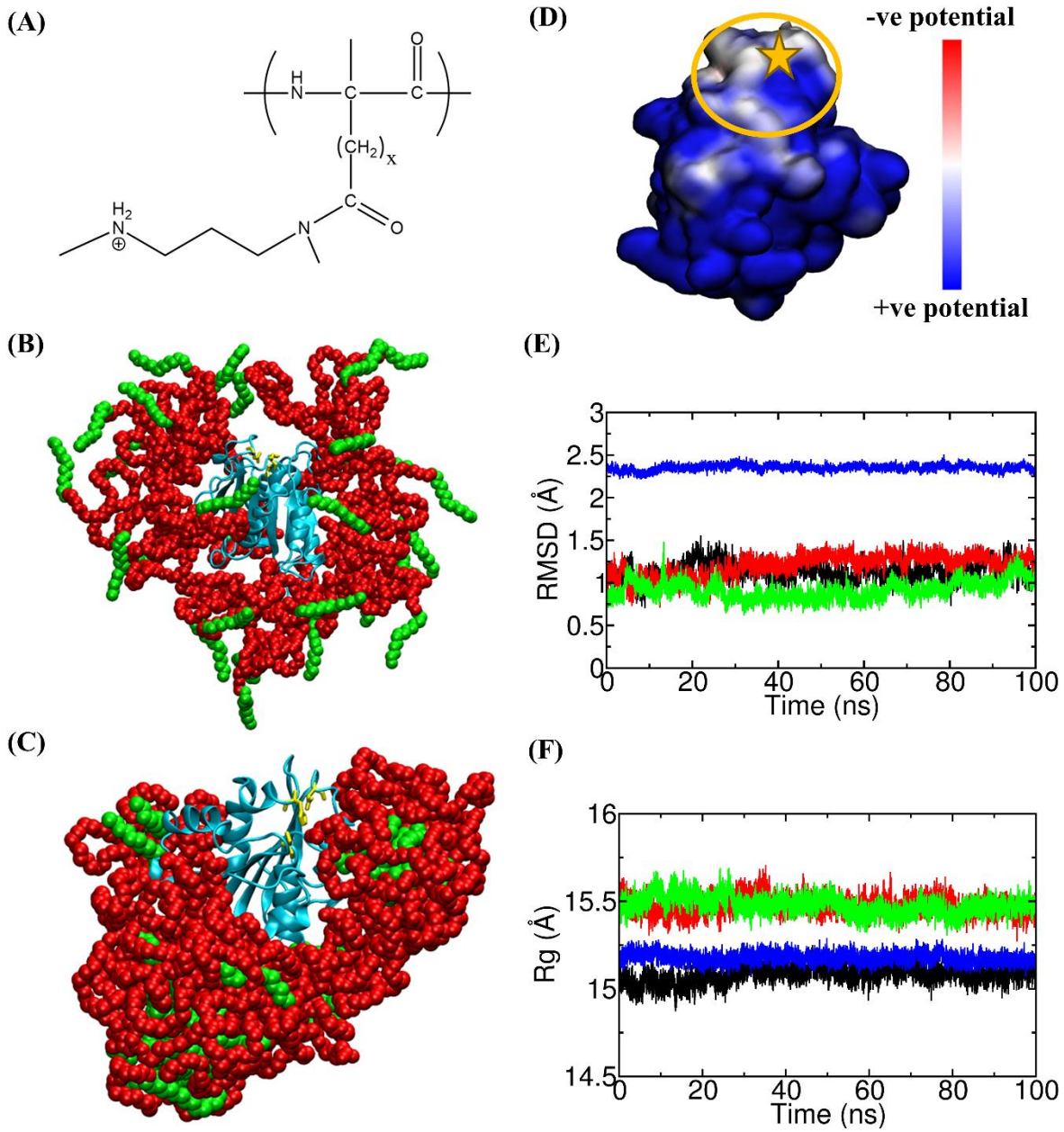

Figure S1. (A) Molecular structures of cationized Aspartate (x=1), Glutamate (x=2), (B) Initial structure for the [cLipA:27S] simulation with all the 27 surfactants placed manually having their carboxylate group pointing toward the positively charged surface sites of cationized LipA (cLipA - Cartoon representation with cyan color, catalytic triad - licorice representation with yellow color, surfactant - vdW representation with red color for head and green color for the tail part), (C) The final structure of [cLipA:27S]. (D) Electrostatic potential map of cationized LipA. Yellow ellipse represents the hydrophobic region of LipA and the position of the active site is marked with an asterisk, (E) Root-mean-square-deviation of atomic position from the crystal structure (all atom), with respect to simulation time for the four different systems; WT LipA (black), cLipA (red), [cLipA:S] (green), SFPL-64 (blue) in one representative MD trajectory, (F) Radius of gyration of the enzyme in all these four systems (same color codes as in (E)).

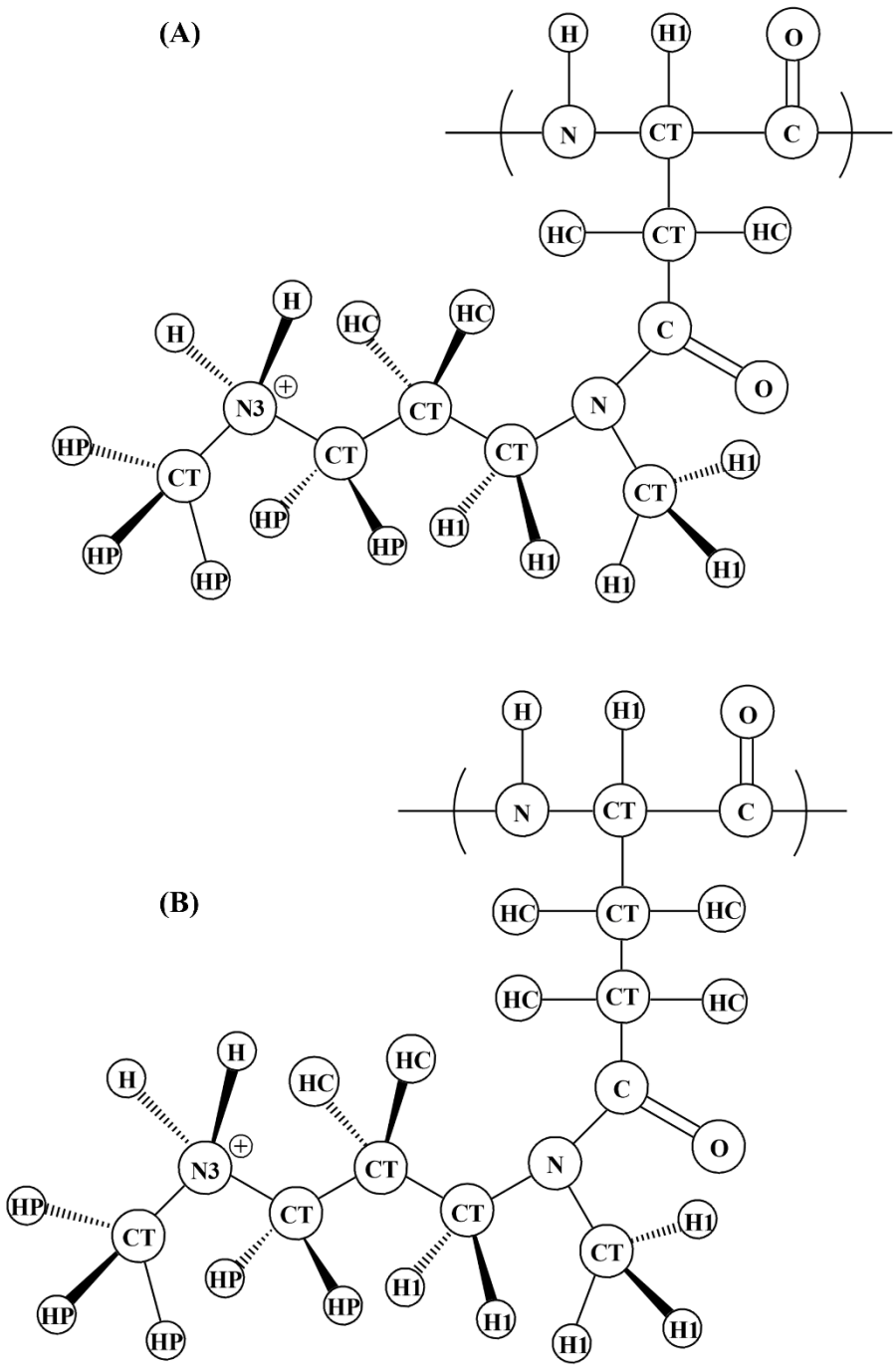

Figure S2. AMBER atom types of (A) cationized aspartate, and (B) cationized glutamate used in the current study.

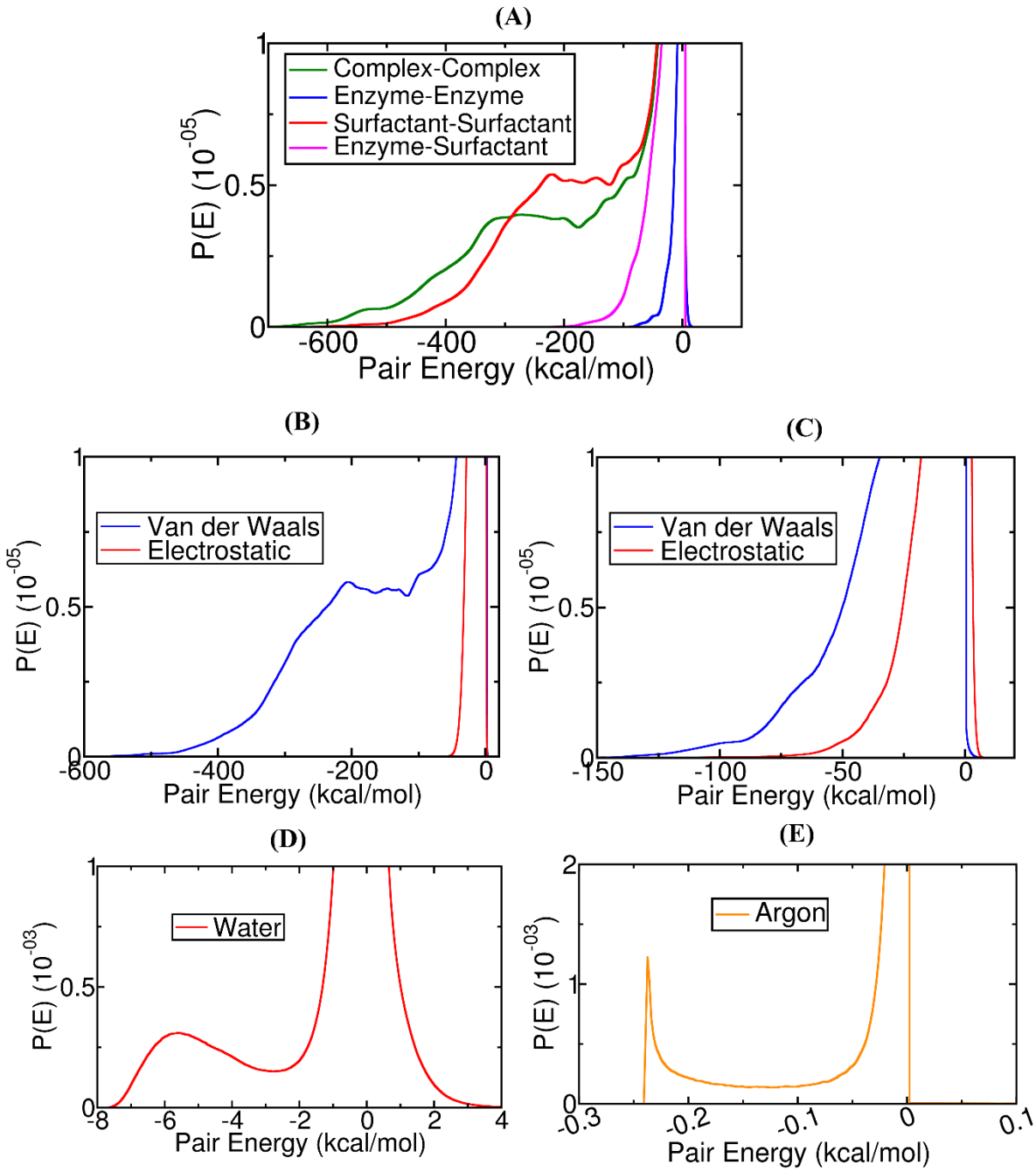

Figure S3. (A) Distribution of pair interaction energies of various pairs in the SFPL. See SI section-1.7 for definitions of different pairs and SI section-3.2 for discussion. The van der Waals and electrostatic contributions to the total pair energy distribution from (B) surfactant-surfactant and (C) enzyme-surfactant interactions. Pair energy distribution of (D) Water and (E) Argon pairs in neat, bulk liquid water (300K, 1 bar) and argon (130K, 40bar) simulations, provided here for the sake of comparison.

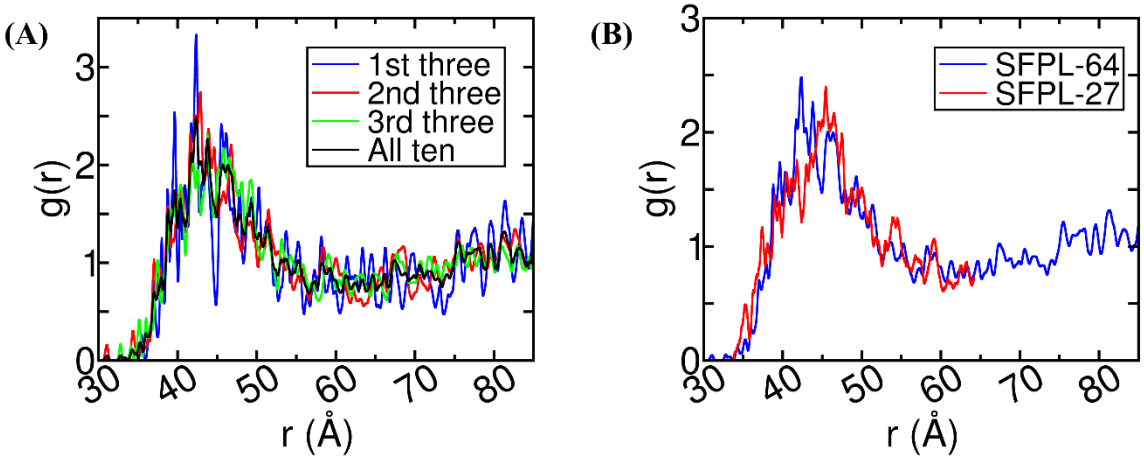

Figure S4. (A) Three P_{com}-P_{com} RDFs (blue, red, and green), each averaged over three (1st three, 2nd three, and 3rd three) independent MD simulation trajectories of SFPL-64 system compared with the RDF mean of all ten configurations from SFPL-64 (B) Comparison of averaged P_{com}-P_{com} RDFs from SFPL-64 and SFPL-27, each averaged over ten independent runs.

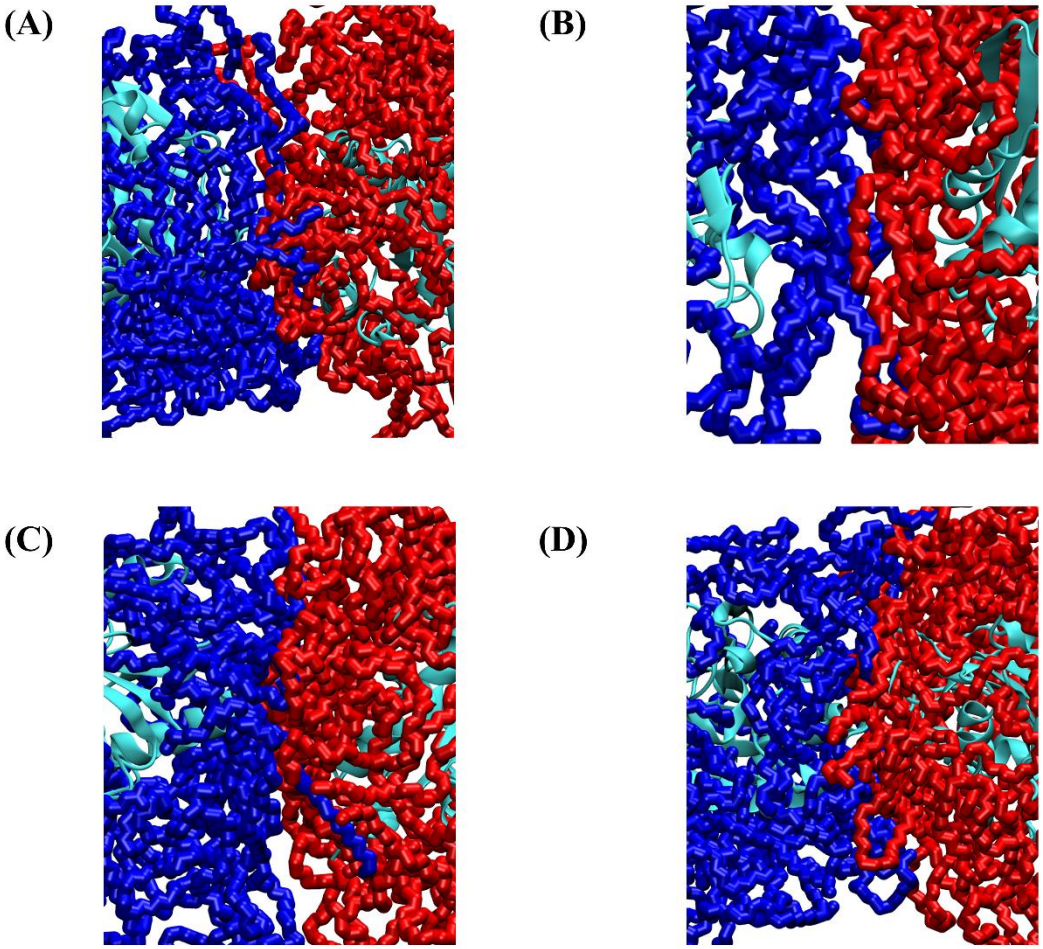

Figure S5. Snapshots of arbitrarily chosen four pairs of enzyme-surfactant complexes, which demonstrate the interdigitation of surfactants (belonging to different complexes). Only a small portion of the enzymes are shown (in cartoon representation with cyan color) so as to focus on the inter-surfactant interactions. The surfactants are shown in licorice representation with blue and red colors for the ones belonging to left and right enzyme-surfactant complexes, respectively.

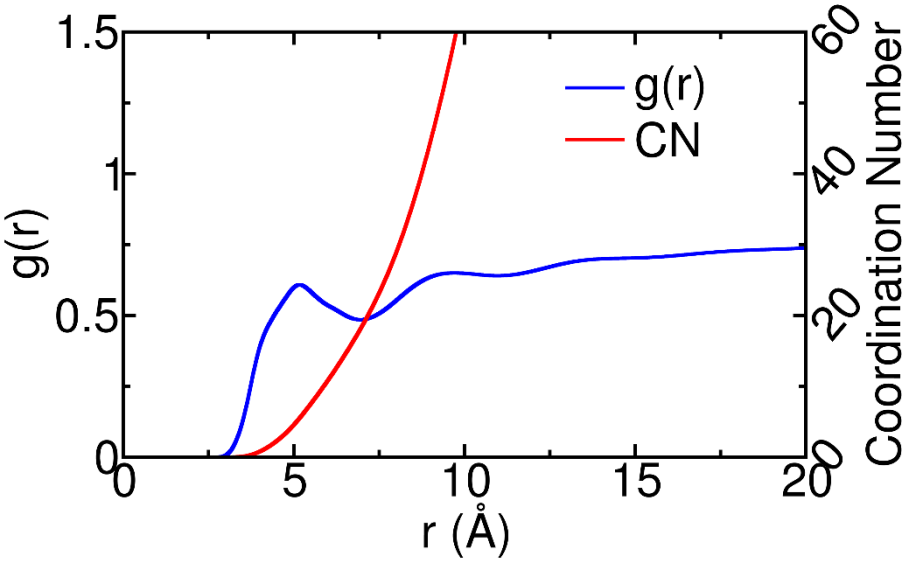

Figure S6. Pair correlation function, g(r) and running coordination number of non-hydrogen atoms of surfactants belonging to different enzyme-surfactant complexes (see SI section 1.7 for definition). The first peak at 5 Å indicates the presence of non-hydrogen atoms of surfactants from other enzyme-surfactant complexes within 5 Å of a non-hydrogen surfactant atom of a particular complex. The coordination number value of 20 in the first coordination shell implies the presence of a substantial number of inter-complex surfactant interactions which agrees well with the interdigitated nature of surfactants (Figure S3) and the high complex-complex pair interaction energy (Figure 2-B of main MS).

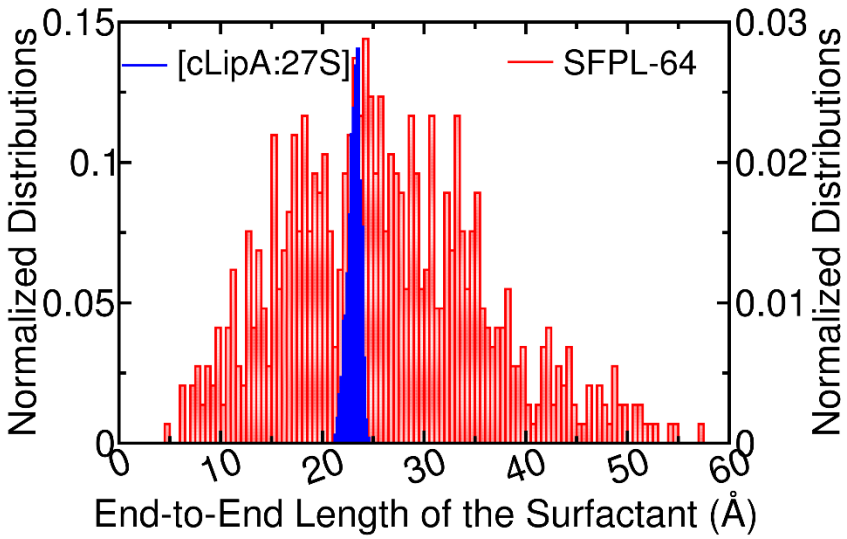

Figure S7. Normalized distribution of the head to tail distance of the surfactant in the SFPL (red, at 333K temperature and 1 bar pressure) and [cLipA:27S] (blue, at 300K temperature and 1 bar pressure).

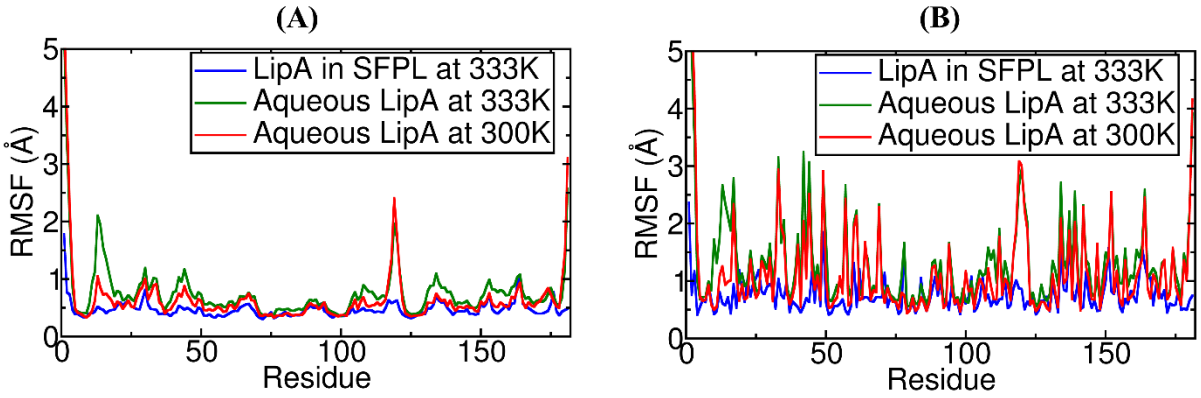

Figure S8. RMSF of (A) backbone atoms and (B) side chain atoms of aqueous LipA and of LipA in SFPL as a function of residue number.

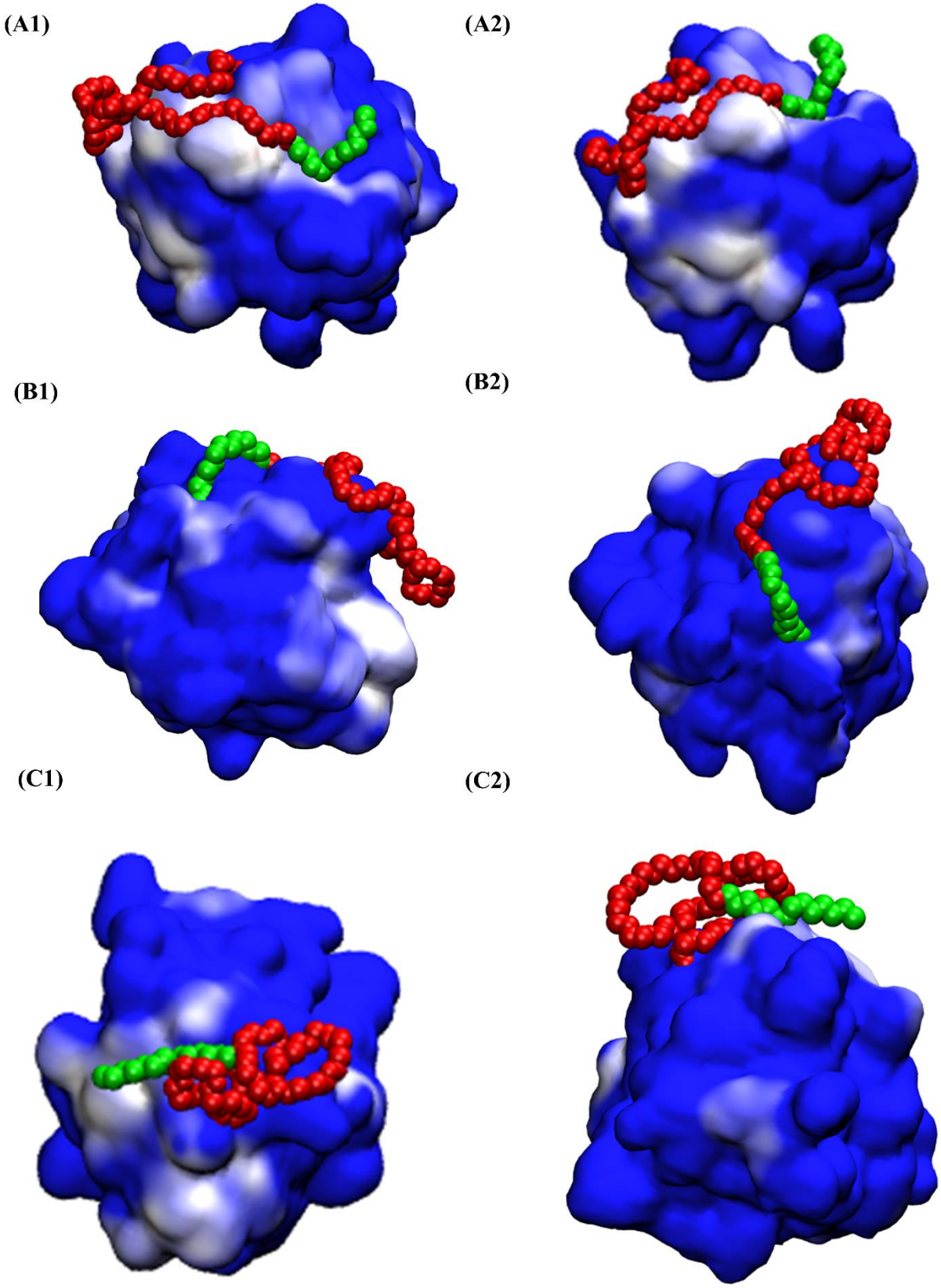

Figure S9. Various snapshots from MD simulations illustrating the interactions of the surfactant (SFT) with the enzyme. (A1) & (A2) are two views showing an alkyl tail of a surfactant interacting with one enzyme. (B1), (B2) and (C1), (C2) are the same for two more alkyl tails. Red spheres are the carboxylate and the PEG parts, while green spheres are the alkyl part of the surfactant.

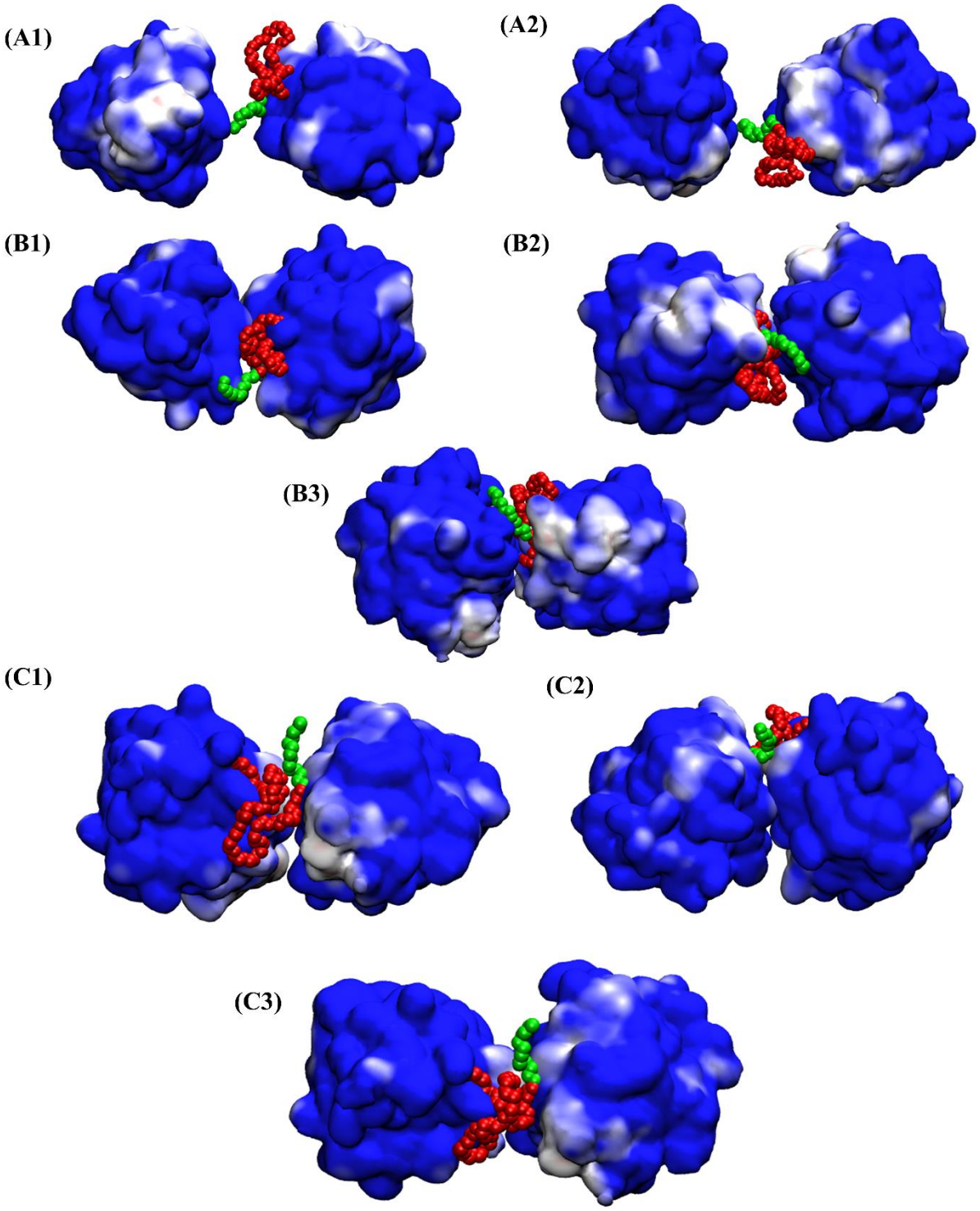

Figure S10. (A1) & (A2): Two views showing an alkyl tail of a surfactant interacting with two enzymes simultaneously. (B1), (B2), (B3) and (C1), (C2), (C3): Three views each of alkyl tails interacting with two enzymes simultaneously. Color codes are the same as in Figure S7.

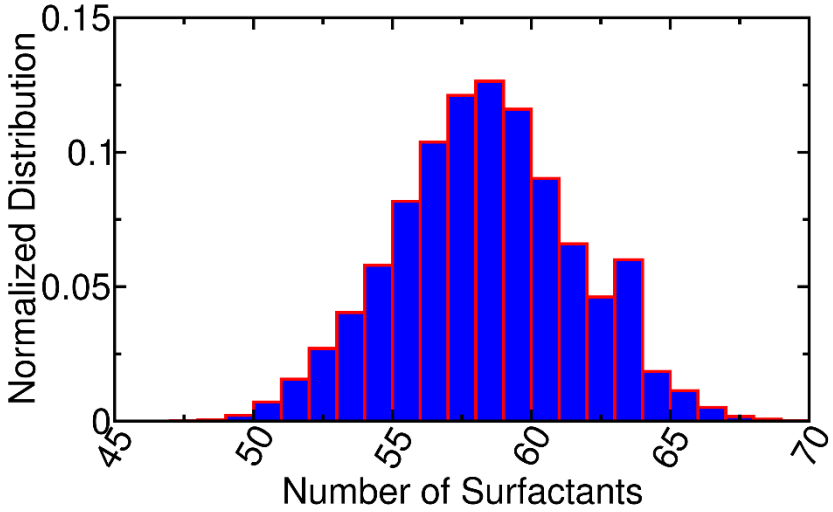

Figure S11. Normalized distribution of the number of surfactants a protein interacts directly with (within 5 Å of a protein). The mean value is 58.

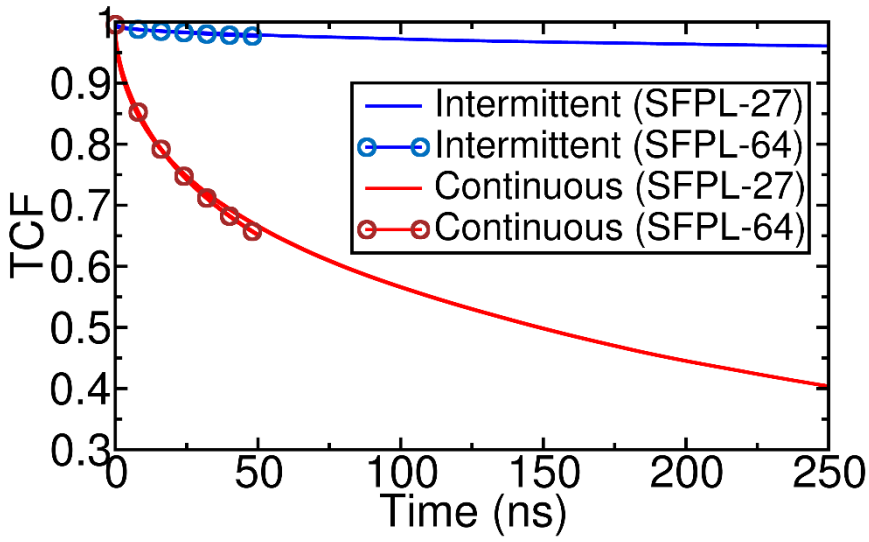

Figure S12. Intermittent and Continuous Lifetime correlation functions of the N-C pair (see main text for definition), calculated from SFPL-27 and SFPL-64, demonstrating identical behavior, despite the relatively shorter trajectory of the latter.

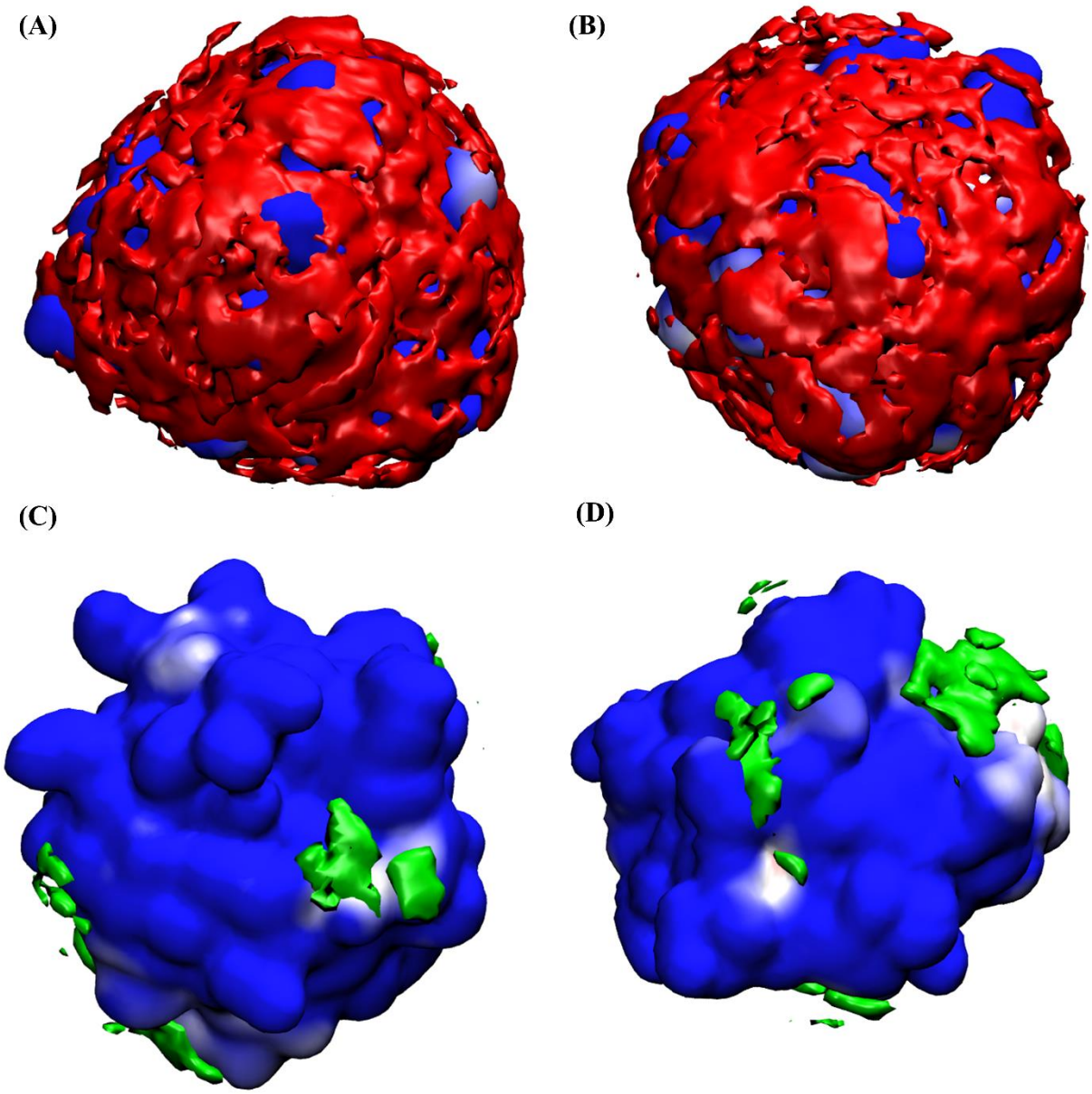

Figure S13. (A) & (B) Two different views showing the density of surfactant's head (PEG+carboxylate, red, isovalue – 0.045 number of non-hydrogen atoms per Å^3) covering the protein surface, (C) & (D) Two different views showing the density of surfactant's alkyl group (green, isovalue – 0.01 number of non-hydrogen atoms per Å^3). The enzyme is shown with its electrostatic potential map (same as in Figure S1D).

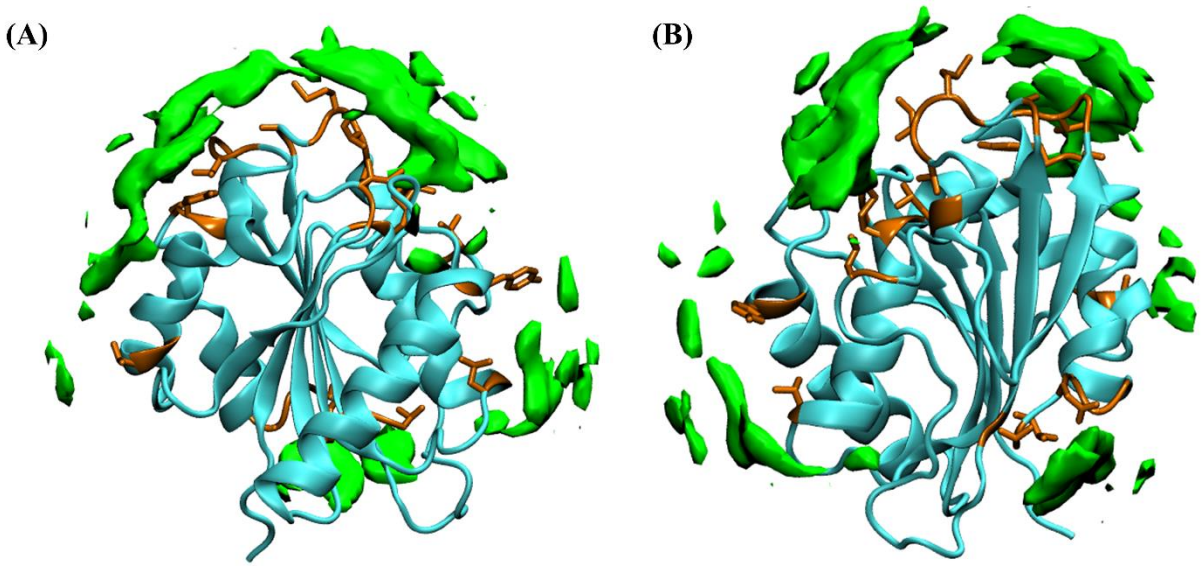

Figure S14. (A), (B) Two different views of protein residues (orange licorice representation), which interact with the carbon atoms of alkyl tails of the surfactants. Alkyl groups are shown as a green isosurface. The enzyme is shown in new cartoon representation with cyan color. Residues which interact with the carbon atoms of alkyl tails of the surfactants are: ILE12, VAL27, TYR49, MET78, LEU90, LEU108, LEU124, ALA132, MET134, ILE135, VAL136, LEU140, GLY153, VAL154, GLY155, TYR161, SER162, GLY176, GLY177, GLN178, and THR180.

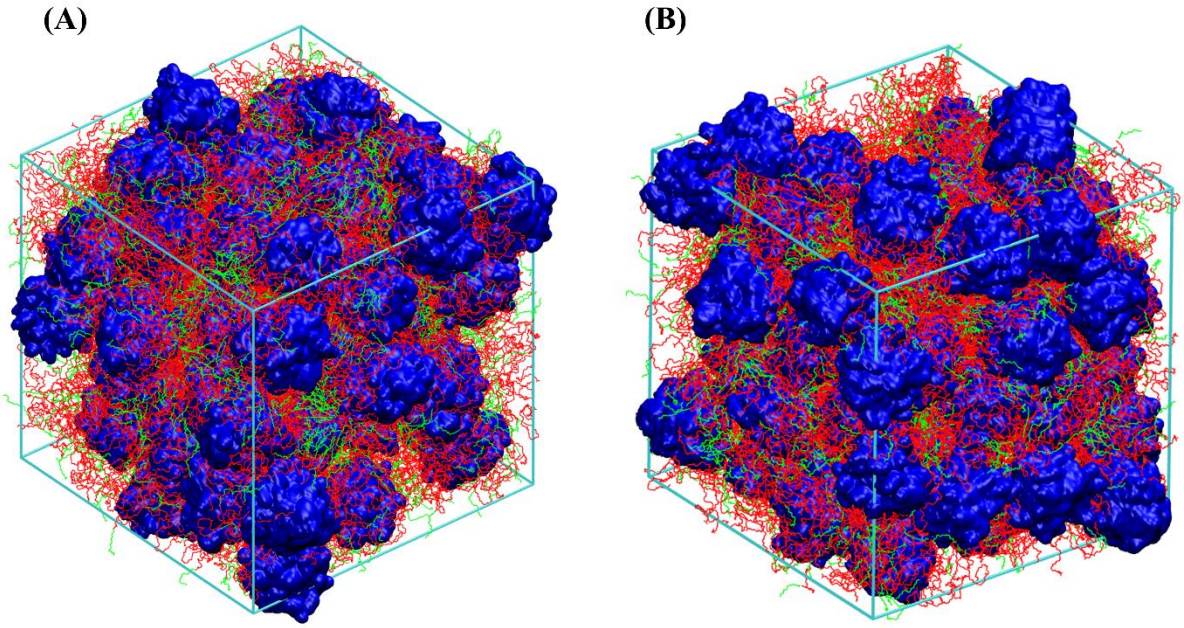

Figure S15. (A), (B) Final configurations at the end of two independent SFPL-64 MD trajectories, viewed from the same orientation as in Figure-4 of the main text. The color scheme is same as in Figure 4 of main manuscript.

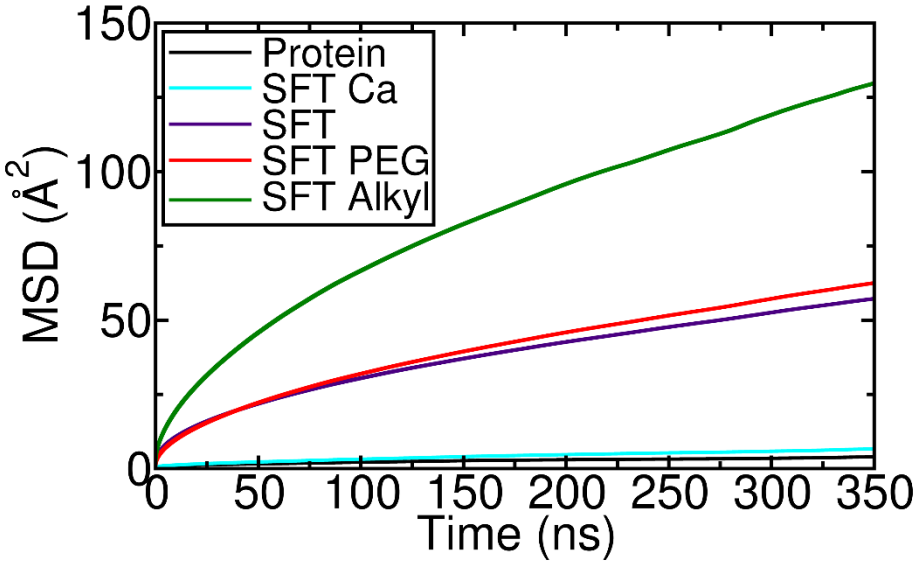

Figure S16. (A) Mean square displacement of protein center of mass (Protein), carboxylate carbon of the surfactant (SFT Ca), COM of the surfactant (SFT), COM of PEG of surfactant (SFT PEG) and COM of alkyl tail of surfactant (SFT Alkyl) obtained from the SFPL-27 simulation.

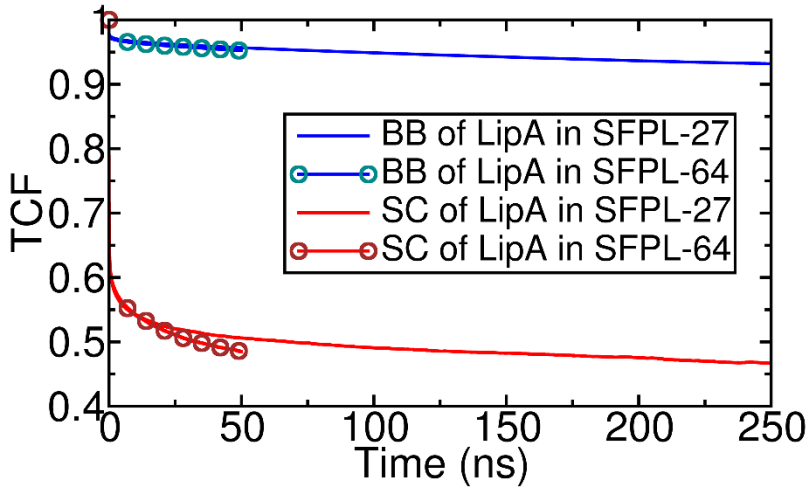

Figure S17. (A) Average TCFs of both side chain and backbone bond vectors of segment-1 (Thr117 to Gln121) showing that the decay of TCFs is similar in both SFPL-64 and SFPL-27.

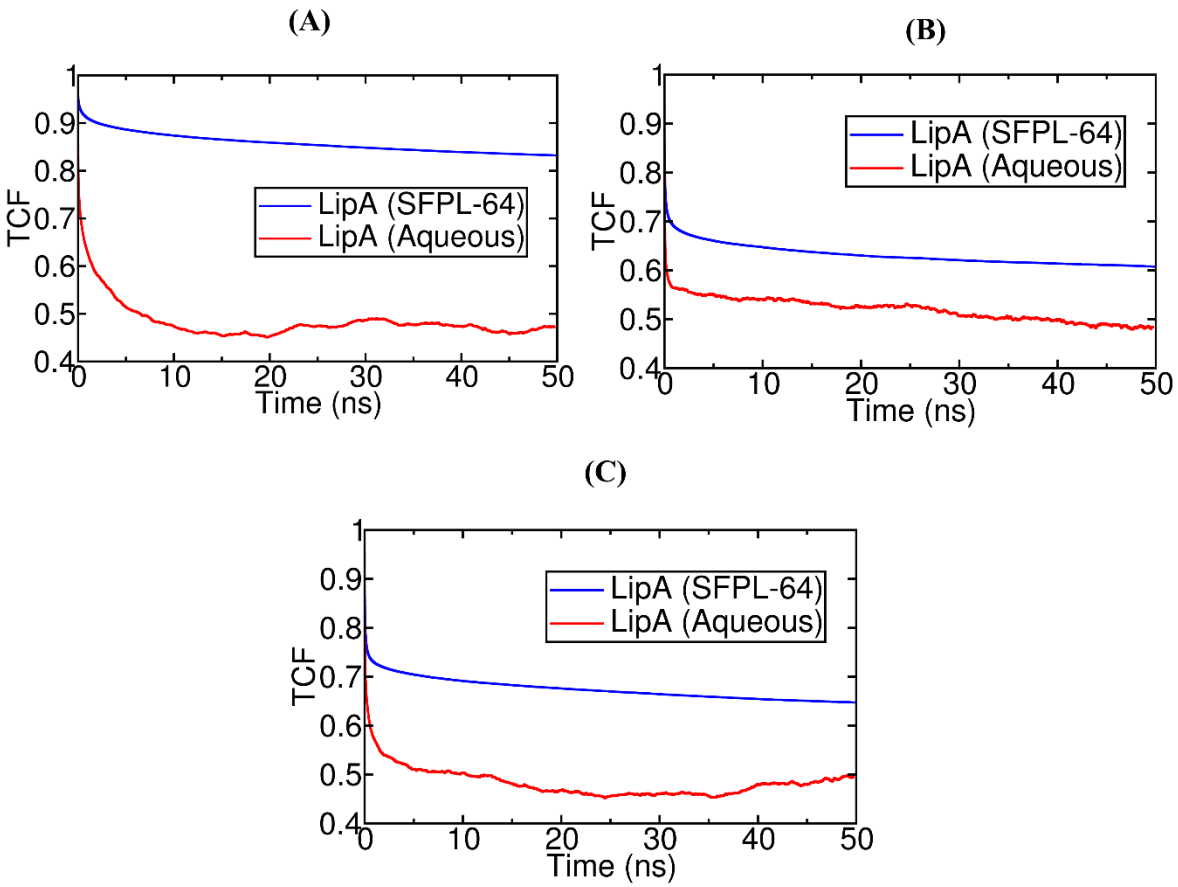

Figure S18. Comparison of the average TCF of side chain bond vectors between the aqueous and SFPL-64 systems of (A) segment-3: Phe41 to Thr47, (B) segment-4: Phe19 to Lys23, and (C) segment-5: Asn148 to His152.

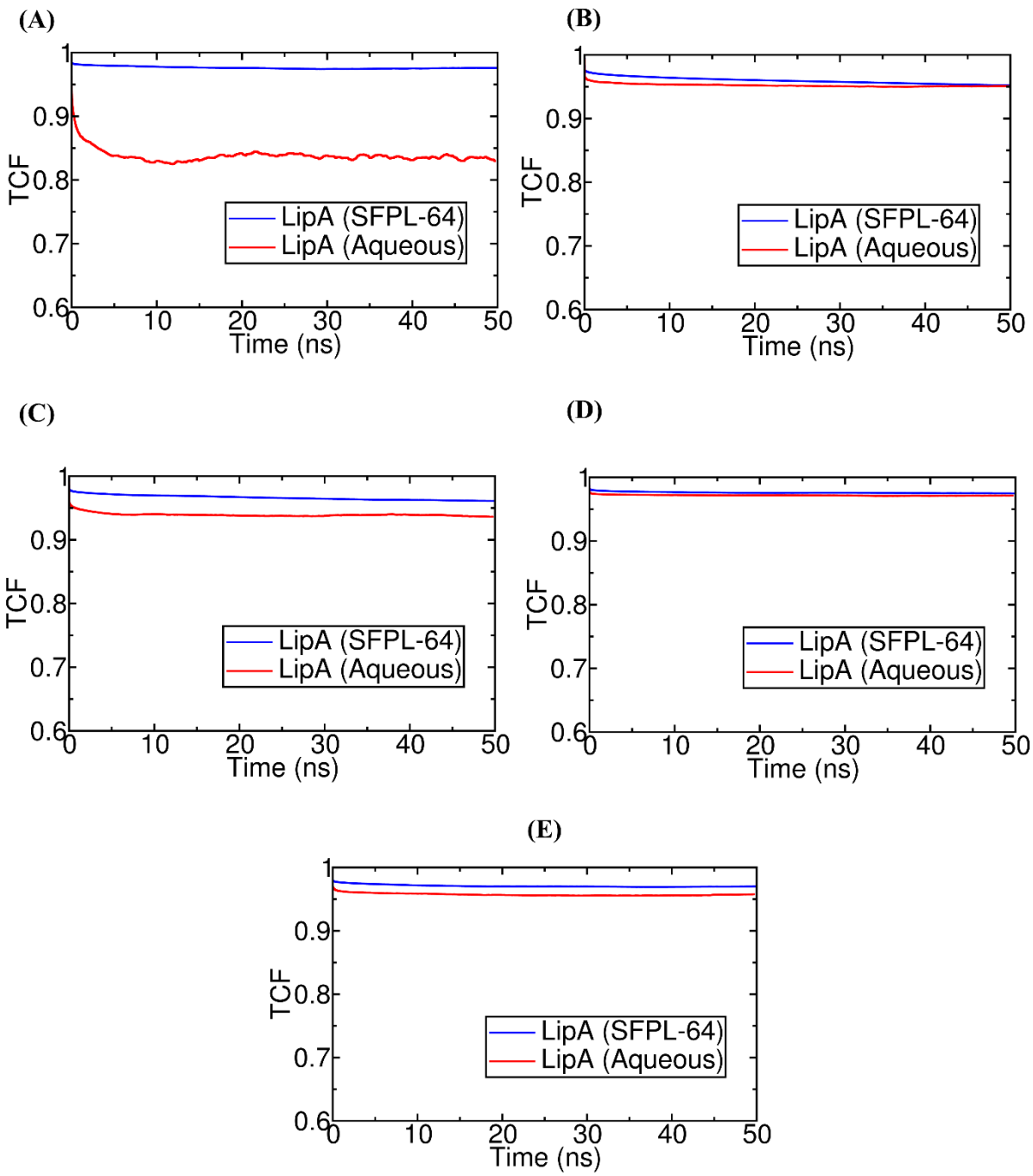

Figure S19. Comparison of the average TCF of backbone bond vectors between the aqueous and SFPL-64 systems of (A) segment-1, (B) segment-2, (C) segment-3, (D) segment-4, and (E) segment-5. The faster decay of TCF of segment-1 in aqueous LipA is due to loop motion (segment-1 is a highly flexible loop), which is restricted in the solvent-free protein liquid.

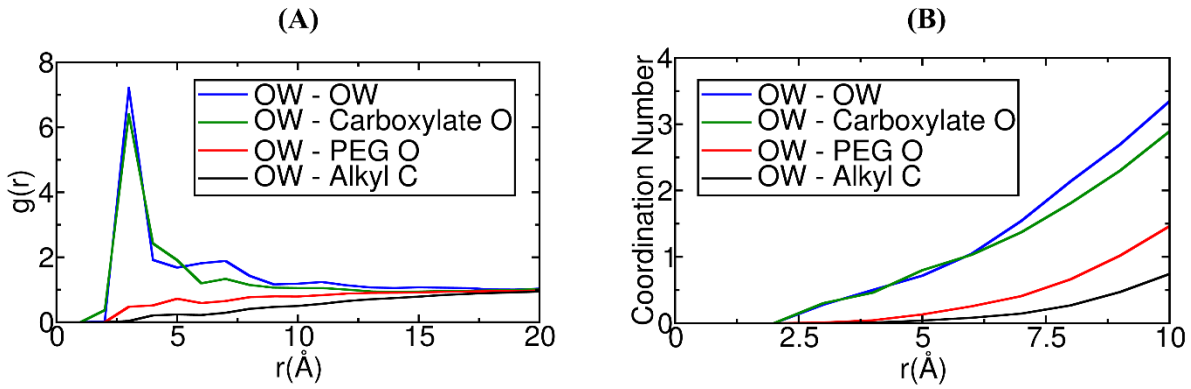

Figure S20. (A) RDFs and (B) Running Coordination numbers of with Oxygen atom of water (OW) with different kinds of atoms (Carboxylate O is oxygen of carboxylate group of the surfactant, PEG O is oxygen of PEG part and Alkyl C is the Carbon of alkyl part of the surfactant) in the SFPL-64.

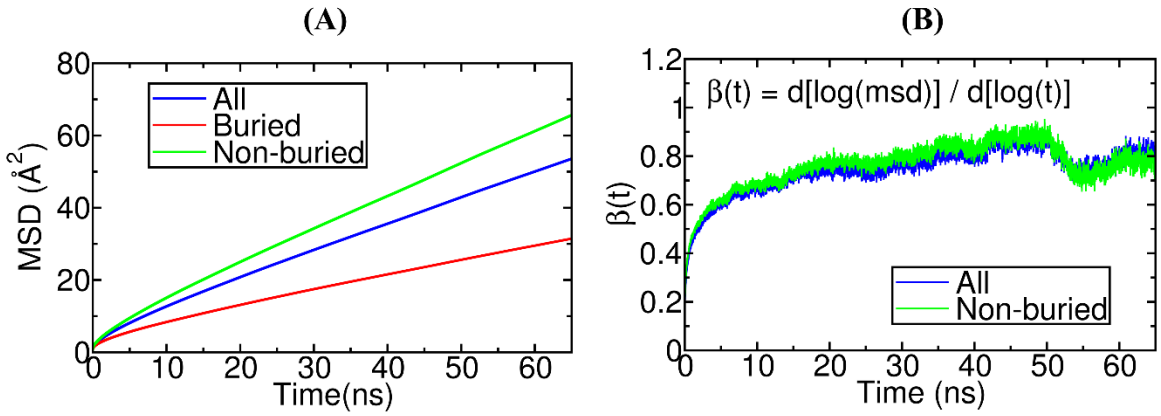

Figure S21. (A) MSDs and (B) β(t) exponent for different types water molecules as a function of time.

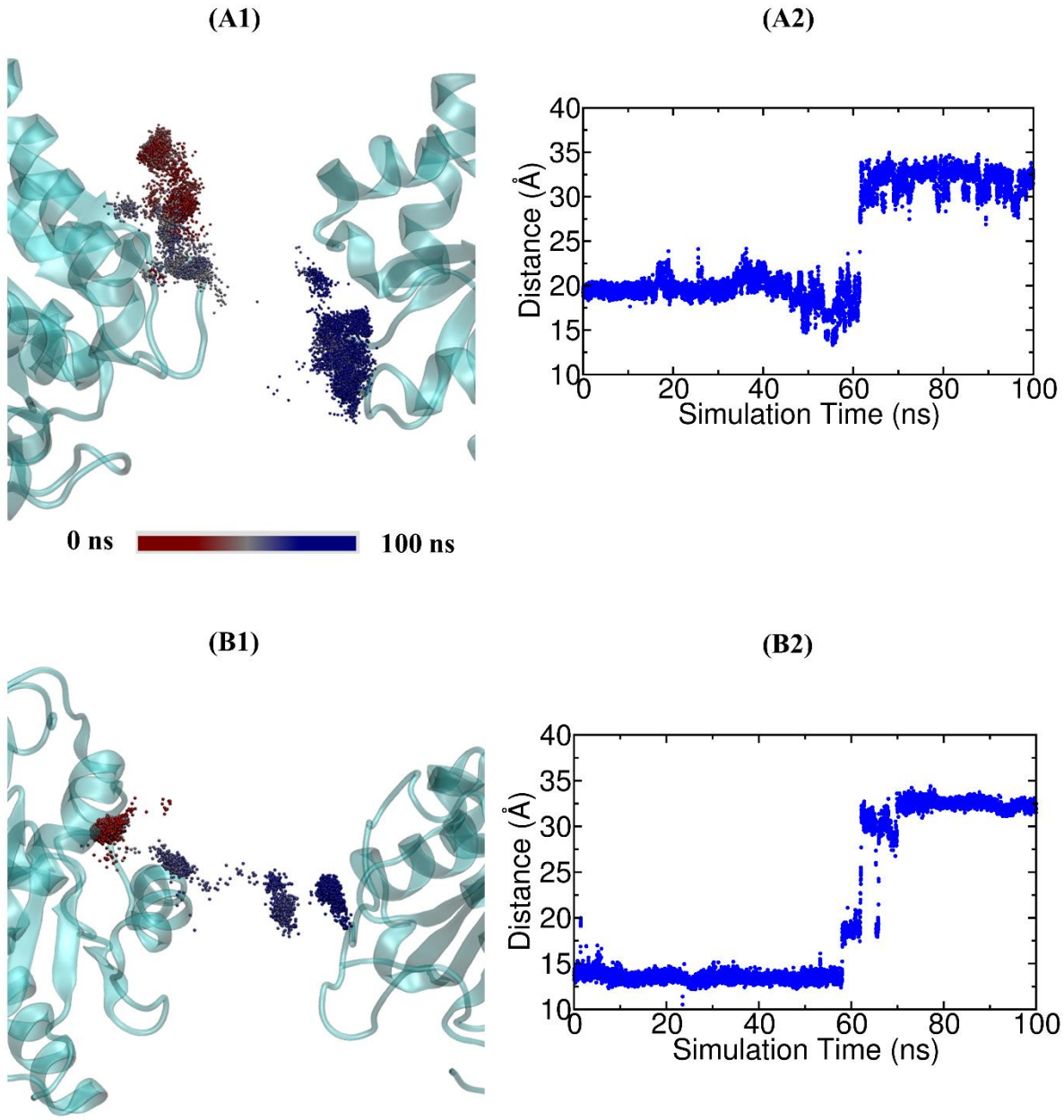

Figure S22. (A1) Trajectory of a specific water molecule (not the same as shown in the main manuscript) shown in dots with a color scale from red (at 0 ns) to blue (at 100 ns) transiting between enzymes. The water molecule transits from one enzyme (on the left) to another (on the right). Enzymes are shown in new cartoon representations with cyan colors. (A2) The distance of the oxygen atom of the same water molecule from the center of mass of the protein on its left. (B1) & (B2) show the same as in (A1) & (A2), respectively, for another water molecule.

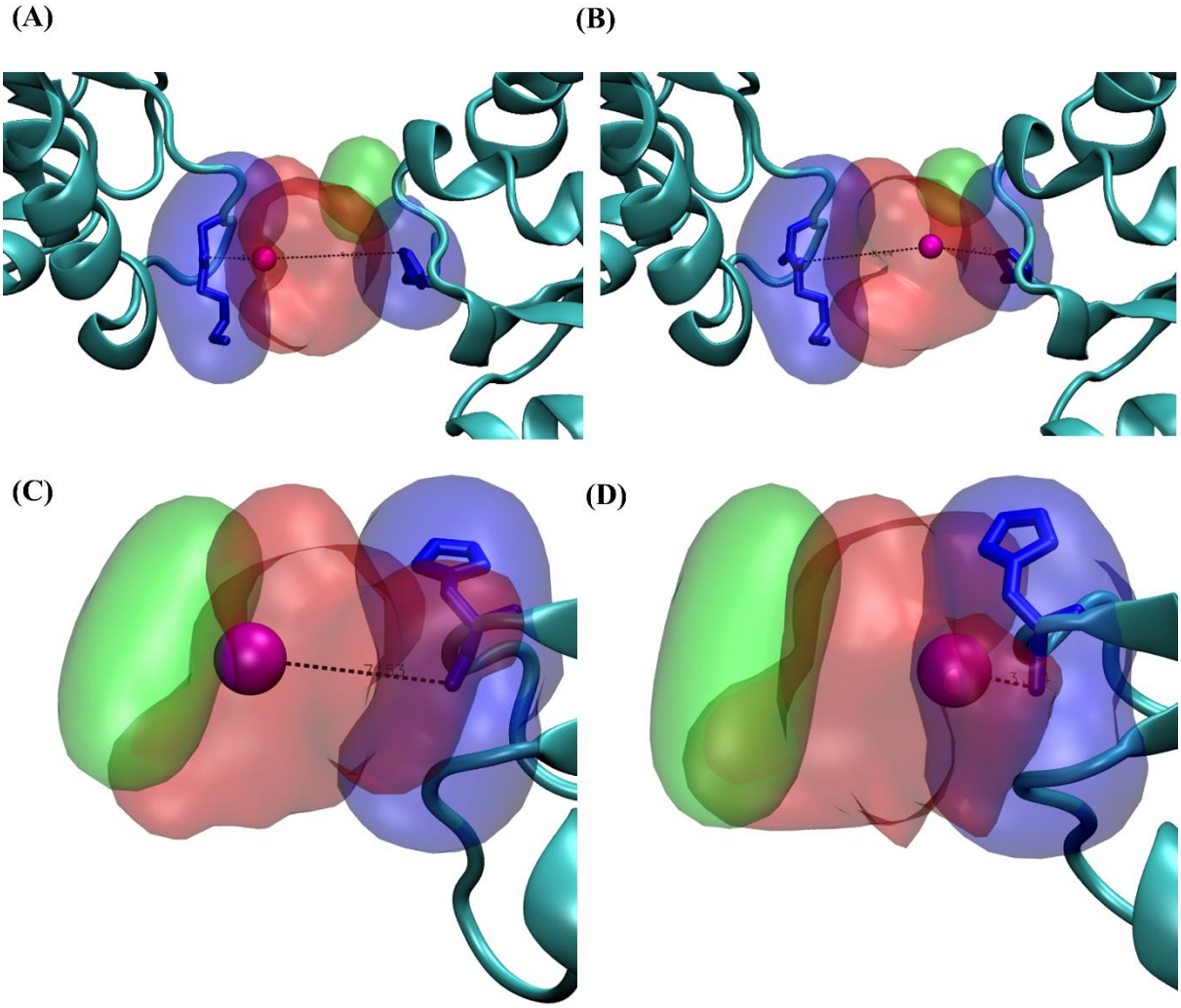

Figure S23. (A-B): Snapshots of the motion of a chosen water molecule which transits between enzymes, to illustrate the atoms that it is interacting with, before and after the 'superfast' motion. Its oxygen atom alone is shown (magenta ball). Both the enzymes are shown in new cartoon representation in cyan color, with one residue from each protein shown in blue licorice representation. The time difference between the two snapshots is 10ps. (A) precedes (B), chronologically. Blue, red, and green transparent surfaces are the non-hydrogen atoms of enzymes, surfactant PEG and surfactant alkyl, respectively, present within 5 Å radius from the line joining the positions of the oxygen atom in these two snapshots. (C-D): Similar figures for another superfast water molecule at two consecutive time frames, separated by 10ps.

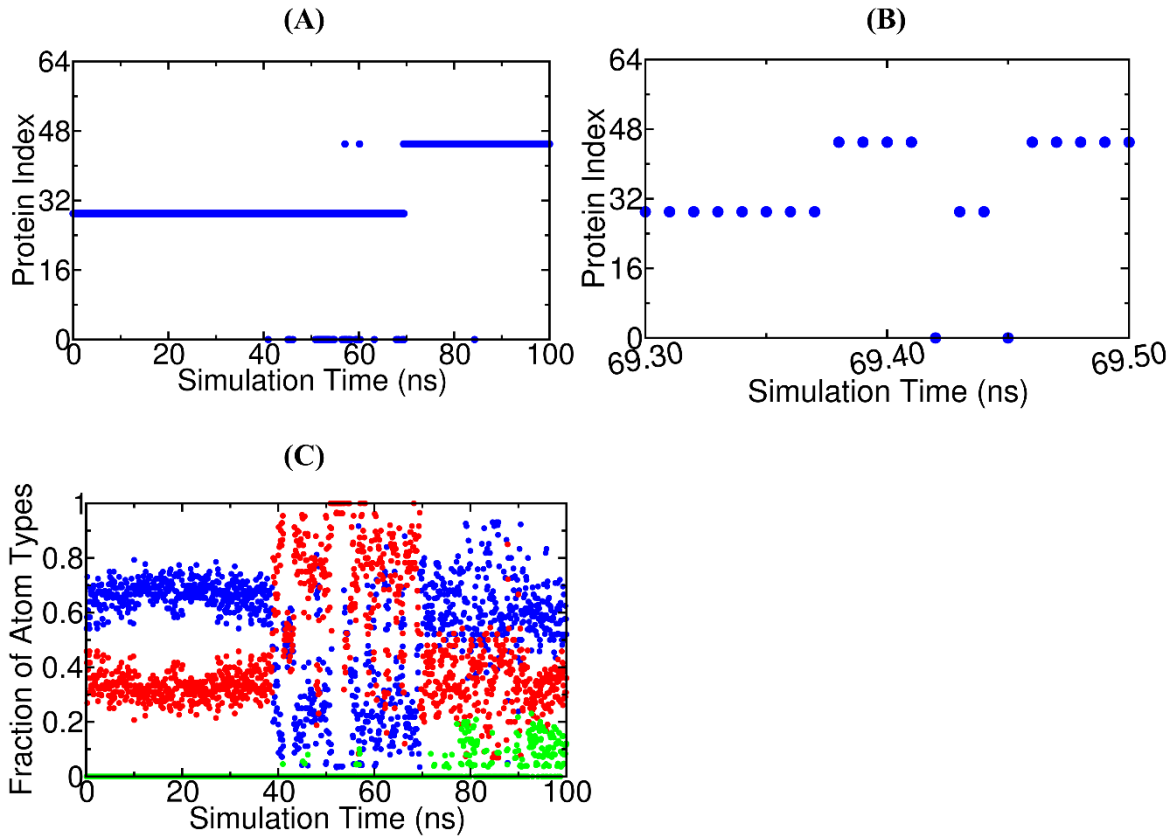

Figure S24. (A) Index of an enzyme with which a specific water molecule is interacting, during the course of the simulation. A protein index 0 means the water molecule is not interacting with any protein and is present in the surfactant medium, (B) Same data as in Panel (A), but zoomed to show the region of transition, which is between 69.30ns and 69.50ns (C) Fraction of neighbor atom types for the specific water molecule shown in Panel (A). Color Scheme: Blue-Protein, Red-SFT head and Green-SFT alkyl.

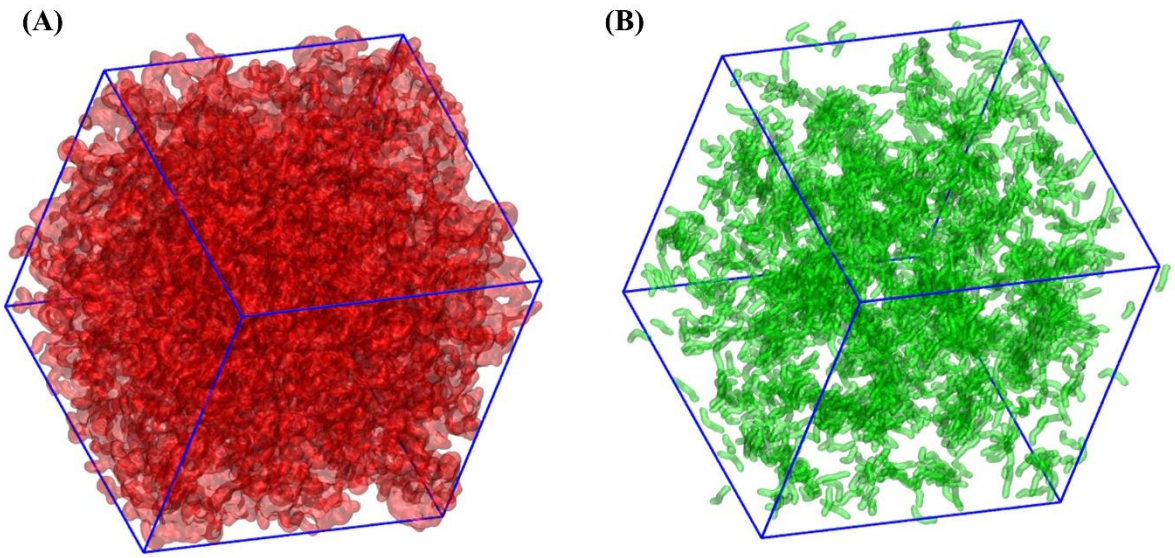

Figure S25. (A) Surfactant head (red) and (B) alkyl groups (green) in the solvent-free protein liquid, shown in QuickSurf representation.

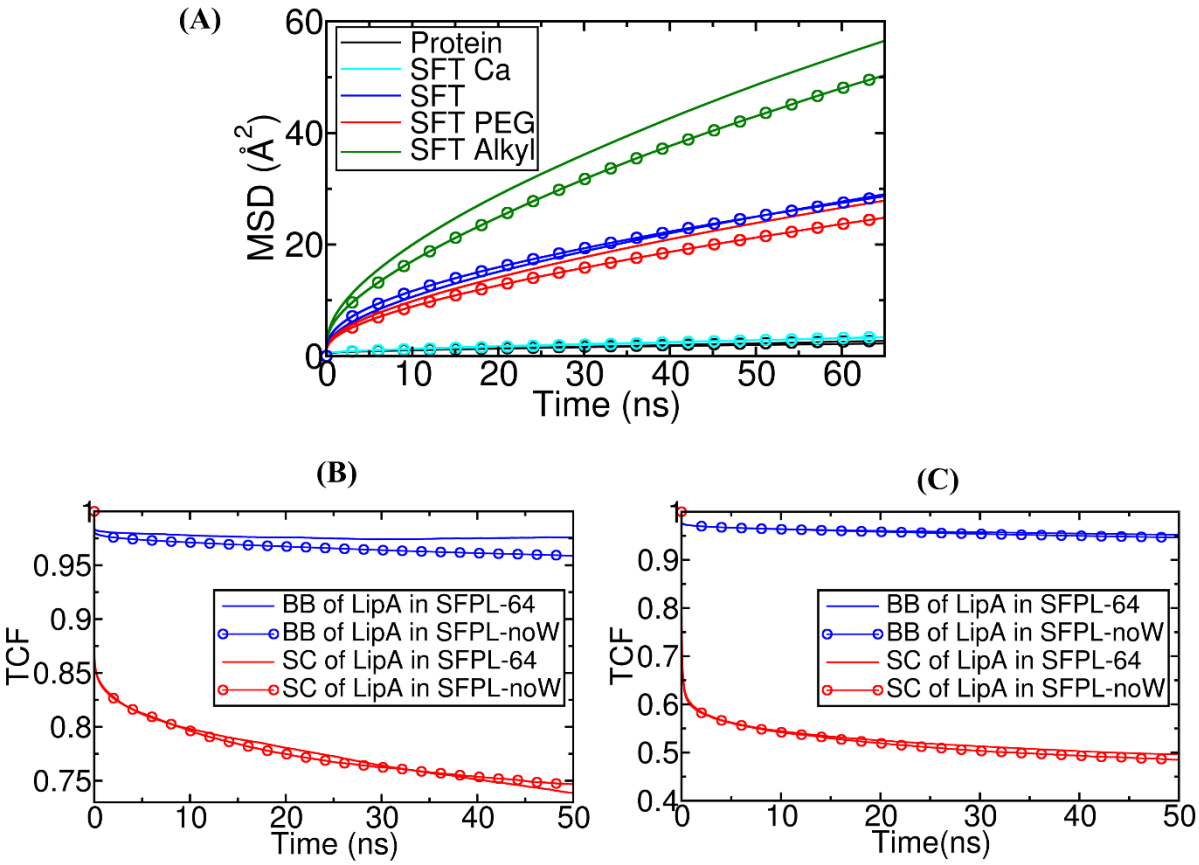

Figure S26. (A) MSD of different parts of the two systems – SFPL-64 (solid line) and SFPL-noW (solid line with circles). Average time correlation functions of bond vectors of the backbone (blue) and side chain (red) bonds of (B) segment-1 and of (C) segment-2 from SFPL-64 and SFPL-noW.

References

1 Y. Zhou, N. C. Jones, J. Nedergaard Pedersen, B. Pérez, S. Vrønning Hoffmann, S. Vang Petersen, J. Skov Pedersen, A. Perriman, P. Kristensen, R. Gao and Z. Guo, *ChemBioChem*, 2019, **20**, 1266–1272.

2 A. P. S. Brogan, R. B. Sessions, A. W. Perriman and S. Mann, *J. Am. Chem. Soc.*, 2014, **136**, 16824–16831.

3 H. J. C. Berendsen, D. van der Spoel and R. van Drunen, *Comput. Phys. Commun.*, 1995, **91**, 43–56.

4 R. Dennington, T. Keith and J. Millam, *Semichem Inc. , Shawnee Mission. KS*, 2009.

5 M. J. Frisch, G. W. Trucks, H. B. Schlegel, G. E. Scuseria, M. A. Robb, J. R. Cheeseman, G. Scalmani, V. Barone, B. Mennucci, G. A. Petersson, H. Nakatsuji, M. Caricato, X. Li, H. P. Hratchian, A. F. Izmaylov, J. Bloino, G. Zheng, J. L. Sonnenberg, M. Hada, M. Ehara, K. Toyota, R. Fukuda, J. Hasegawa, M. Ishida, T. Nakajima, Y. Honda, O. Kitao, H. Nakai, T. Vreven, J. A. Montgomery, J. E. Peralta, F. Ogliaro, M. Bearpark, J. J. Heyd, E. Brothers, K. N. Kudin, V. N. Staroverov, R. Kobayashi, J. Normand, K. Raghavachari, A. Rendell, J. C. Burant, S. S. Iyengar, J. Tomasi, M. Cossi, N. Rega, J. M. Millam, M. Klene, J. E. Knox, J. B. Cross, V. Bakken, C. Adamo, J. Jaramillo, R. Gomperts, R. E. Stratmann, O. Yazyev, A. J. Austin, R. Cammi, C. Pomelli, J. W. Ochterski, R. L. Martin, K. Morokuma, V. G. Zakrzewski, G. A. Voth, P. Salvador, J. J. Dannenberg, S. Dapprich, A. D. Daniels, Farkas, J. B. Foresman, J. V Ortiz, J. Cioslowski and D. J. Fox, *Gaussian 09, Revis. B.01, Gaussian, Inc., Wallingford CT*, 2009.

6 J. Wang, R. M. Wolf, J. W. Caldwell, P. A. Kollman and D. A. Case, *J. Comput. Chem.*, 2004, **25**, 1157–1174.

7 C. I. Bayly, P. Cieplak, W. D. Cornell and P. A. Kollman, *J. Phys. Chem.*, 1993, **97**, 10269–10280.

8 J. Wang, W. Wang, P. a Kollman and D. a Case, *J. Am. Chem. Soc*, 2001, **222**, U403.

9 A. W. Sousa Da Silva and W. F. Vranken, *BMC Res. Notes*, , DOI:10.1186/1756-0500-5-367.

10 D. J. Price and C. L. Brooks, *J. Chem. Phys.*, 2004, **121**, 10096–10103.

11 N. Michaud-Agrawal, E. J. Denning, T. B. Woolf and O. Beckstein, *J. Comput. Chem.*, 2011, **32**, 2319–2327.

12 K. Lindorff-Larsen, S. Piana, K. Palmo, P. Maragakis, J. L. Klepeis, R. O. Dror and D. E. Shaw, *Proteins Struct. Funct. Bioinforma.*, 2010, **78**, 1950–1958.

13 J. H. Lee, K. Pollert and L. Konermann, *J. Phys. Chem. B*, 2019, **123**, 6705–6715.

14 D. S. Cerutti, P. L. Freddolino, R. E. Duke and D. A. Case, *J. Phys. Chem. B*, 2010, **114**, 12811–12824.

15 W. Humphrey, A. Dalke and K. Schulten, *J. Mol. Graph.*, 1996, **14**, 33–38.

16 R. Fletcher, *Comput. J.*, 1964, **7**, 149–154.

17 W. F. Van Gunsteren and H. J. C. Berendsen, *Mol. Simul.*, 1988, **1**, 173–185.

18 G. Bussi, D. Donadio and M. Parrinello, *J. Chem. Phys.*, , DOI:10.1063/1.2408420.

19 H. J. C. Berendsen, J. P. M. Postma, W. F. Van Gunsteren, A. Dinola and J. R. Haak, *J. Chem. Phys.*, 1984, **81**, 3684–3690.

20 S. Nosé and M. L. Klein, *Mol. Phys.*, 1983, **50**, 1055–1076.

21 B. Hess, H. Bekker, H. J. C. Berendsen and J. G. E. M. Fraaije, *J. Comput. Chem.*, 1997, **18**, 1463–1472.

22 T. Darden, D. York and L. Pedersen, *J. Chem. Phys.*, 1993, **98**, 10089–10092.

23 N. A. Baker, D. Sept, S. Joseph, M. J. Holst and J. A. McCammon, *Proc. Natl. Acad. Sci. U. S. A.*, 2001, **98**, 10037–10041.

24 A. Rahman and F. H. Stillinger, *J. Chem. Phys.*, 1971, **55**, 3442–3449.